

Predictive control of a general water distribution system by using sequential linear programming

Korotaj, Blaž; Vašak, Mario

Source / Izvornik: **Control Engineering Practice, 2025, 156**

Journal article, Published version

Rad u časopisu, Objavljena verzija rada (izdavačev PDF)

<https://doi.org/10.1016/j.conengprac.2024.106232>

Permanent link / Trajna poveznica: <https://urn.nsk.hr/urn:nbn:hr:168:781646>

Rights / Prava: [Attribution 4.0 International](#)/[Imenovanje 4.0 međunarodna](#)

Download date / Datum preuzimanja: **2025-03-28**



Repository / Repozitorij:

[FER Repository - University of Zagreb Faculty of Electrical Engineering and Computing repository](#)





Predictive control of a general water distribution system by using sequential linear programming[☆]

Blaž Korotaj^{ID}*, Mario Vašak^{ID}

University of Zagreb Faculty of Electrical Engineering and Computing, Laboratory for Renewable Energy Systems, Unska 3, 10000 Zagreb, Croatia

ARTICLE INFO

Keywords:

Water distribution system
Predictive control
Sequential linear program
General network
Linearization

ABSTRACT

The paper focusses on water distribution systems (WDSs) of a general configuration, whose operation profile is decided by solving a sequential linear program (SLP). The paper introduces linearization procedure for a general network. The necessary SLP mathematical form for a general WDS is also derived. Cost function and all the constraints for the WDS optimization are elaborated. To validate the approach, the derived procedure is applied to a toy example and to a large segment of a WDS from a city in Spain. The results are compared with the operation policy obtained using hysteresis control and substantial operational costs reduction possibilities are demonstrated while respecting all WDS constraints.

1. Introduction

Water distribution operators are looking for advanced water delivery strategies which bring energy-efficient and reliable solutions for consumers (Martinez, Puig, Cembrano, & Quevedo, 2013). In the face of rising complexity, future urban water delivery systems will require increasingly sophisticated technologies to perform reliably and effectively (Berkel, Caba, Bleich, & Liu, 2018). Water flow manipulators (pumps and valves) have been used to maximize a variety of objectives in water networks, including production and transportation costs, water quality, safe storage, smooth control actions, and so on (Fooladivanda & Taylor, 2018). Further, as network topology complexity grows (Archibald & Marshall, 2018), small perturbations can cause significant performance decrease and even infeasibility of optimal water flow problems (Goryashko & Nemirovski, 2014).

Optimal control in water networks deals with the problem of planning control inputs ahead of time, which adhere to all operational constraints, while they achieve certain performance goals. They may include one or more of the following, according to the needs of a specific utility: minimization of supply and pumping costs, maximization of water quality, pressure regulation for leaks reduction, etc. (Cembrano, Wells, Quevedo, Pérez, & Argelaguet, 2000). Model predictive control (MPC), or receding horizon control, is a well-established method of achieving optimal control (Rawlings, Mayne, & Diehl, 2017) and is

increasingly applied to Water Distribution Systems (WDSs) (Engell, 2007) to improve operations in dynamic water demand conditions while respecting all requirements and minimizing costs (Abdulrahman & Nasher, 2010). The WDS model is inherently nonlinear because of the nonlinear relationship between flow and pressure difference on WDS elements, as a consequence of basic Bernoulli law of hydrodynamics. To effectively control the system over a wide operating area, it is necessary to utilize MPC with a nonlinear model. An attempt to take the pressure/head model into account in the flow-based MPC is made in Sun, Puig, and Cembrano (2014), where the non-linear constraints from the flow-head equations are used to update the operational constraints of tanks and actuators by solving a constraint satisfaction problem prior to solving the flow-based linear MPC problem. Again, it was also demonstrated that MPC with a nonlinear model is significantly more computationally expensive compared to when a linear model is used, making it challenging for implementation in a time-sensitive setting.

In Cembrano et al. (2000), the authors described an approach to optimal control in water distribution networks, developing an optimal control tool and demonstrating its application to the city of Sintra, Portugal. Furthermore, connection with other water management tools, such as modelling and quality control programs, ensures feasible and dependable solution. The latter research highlights that complex networks, especially those with mesh structures, impose a high computational burden. Optimization becomes challenging for large,

[☆] This work was supported by the European Union via Horizon 2020 programme through the project Resilient Water Innovation for Smart Economy (REWAISE, Grant agreement ID: 869496). The work has also been supported by the Croatian Science Foundation through the Young Researchers' Career Development Project - Training New Doctoral Students under contract No. DOK-2020-01-4118 and by the European Regional Development Fund through the project Predictive Control for Efficient and Flexible Water Distribution System Operation (Dodola, project code NPOO.C3.2.R3-I1.04.0149).

* Corresponding author.

E-mail addresses: blaz.korotaj@fer.unizg.hr (B. Korotaj), mario.vasak@fer.unizg.hr (M. Vašak).

<https://doi.org/10.1016/j.conengprac.2024.106232>

Received 8 August 2024; Received in revised form 25 December 2024; Accepted 27 December 2024

Available online 8 January 2025

0967-0661/© 2025 The Authors. Published by Elsevier Ltd. This is an open access article under the CC BY license (<http://creativecommons.org/licenses/by/4.0/>).

interconnected water distribution networks with multiple reservoirs and pumps. Simplifications, such as removing small-diameter pipes or low-capacity reservoirs, are required, which may impact model accuracy. In Wang, Ocampo-Martinez, and Puig (2015), authors successfully implemented the MPC strategy in the WDS using a control-oriented model that only takes flows into account. Accordingly, the explicit consideration of the pressures of each WDS element, including storage tanks, demand sectors, pipes, pumps, pressure-controlled valves and flow-controlled valves is omitted. For a certain WDS, it is necessary to adhere to minimum pressure limits at each sector's water demand point and in specific control points in addition.

In previous research, water distribution networks were often also abstracted and simplified since the corresponding optimal control calculations, and even just the simulations of the network hydraulic model, were complex. In Baunsgaard, Ravn, Kallesøe, and Poulsen (2016), the authors introduced a WDS model and a MPC procedure for a network that includes only the fundamental components of a distribution system. However, they did not propose a general approach for advanced control solutions in the context of a broader distribution system network. Furthermore, in Ciminski and Duzinkiewicz (2017) MPC is applied to WDS of the Chojnice city (Poland) based on a genetic algorithm. The primary shortcomings here are the difficulty in identifying an appropriate fitness function, selecting the various parameters, and execution time. While the described procedure in Ciminski and Duzinkiewicz (2017) can be extended to larger WDS scales, it is important to note that these shortcomings become more prominent in such cases and may lead to infeasible solutions. Furthermore, the approach in Shao, Zhou, Yu, Zhang, and Chul (2024) based on linearization and converting a mixed-integer nonlinear program (MINLP) into a mixed-integer linear program (MILP) in a large-scale WDS results in nearly 10% energy savings compared to the genetic algorithm. The drawback of this approach is that the presence of complicated loops leads to increased model-reality flows discrepancies, posing a potential issue in realistic large-scale WDSs. Another approach of transformation of the original MINLP into a MILP through linearization in Vieira, Mayerle, Campos, and Coelho (2020) not only cuts down the service provider's costs by over 16%, but also results in over 27% reduction in losses. An additional positive outcome of the provided solution is a nearly 17% decrease in energy consumption. Despite this transformation, the primary challenge remains the execution time, which hinders the practical application of this method to real systems.

The research presented in Menke, Abraham, Parpas, and Stoianov (2016), which focuses on demand response, illustrates that across various electricity tariffs and water demand scenarios, there are demand response mechanisms that enable the WDS to offer demand response capabilities. This not only lowers its operational costs but also provides broader benefits in terms of green energy share increase and thus further reinforced greenhouse emissions reduction based on optimal control. One of the shortcomings in that research is that the WDS was modelled using quasi-steady-state modelling.

The approach in this research is based on simulation of the full WDS nonlinear model using the open-source tool EPANET (Rossman, Woo, Tryby, Shang, Janke, & Haxton, 2020) for simulating the hydraulics of a complex WDS. Through simulation, a sequence of operational points is obtained around which the WDS nonlinear model is then linearized. The obtained linear models are used to formulate a linear program for improvement of WDS operation via an optimized perturbation of WDS commands. Around the perturbed and improved response these steps are repeatedly applied in a Sequential Linear Program (SLP) procedure. The procedure is functional for complex distribution systems of a general configuration without a need for any abstraction or simplification of the network. Also, this approach does not encounter computational issues with complicated loops on large-scale networks and remains computationally efficient even on an average personal computer, unlike the previously mentioned studies. For that purpose a new method for modelling and linearizing the general distribution network is here

introduced and described. The approach is first validated on a toy-example and then applied to a large WDS segment of a city in Spain. The introduced approach leads to significant cost savings compared to baseline management methods in real-world WDSs.

Main paper contributions are the following:

- A mathematical approach to solving a general water distribution network via virtual cuts without any simplifying assumptions regarding its structure.
- Sequential linear program for optimization of a water distribution system operation.
- Derived procedures verified on a large-scale system indicating high gains in use.

The paper is structured as follows: Section 2 describes a general WDS setup; WDS optimization approach is explained in Section 3; Section 4 describes SLP for a WDS; Optimization results for the toy example and the real WDS segment case studies are reported in Section 5; and Section 6 concludes the paper.

2. A general WDS setup considered

A WDS consists of storages, pressure- and flow-driven pumps, pressure breaker valves (PBVs) and pipes. Its role is to deliver drinking water from the drinking water treatment plant (DWTP) to the end-customers, under proper pressure conditions for a wide range of water demands that the end-users generate. In this research, a general water distribution network setup is being considered without any simplifications. There is no limit to the number of the network components. Let the network consist of a set of nodes \mathcal{N} indexed with integers and a set of branches \mathcal{B} connecting two neighbouring nodes. The branches are ordered pairs (m, n) , $m < n$, $m, n \in \mathcal{N}$, also indexed with integers b . A subset of all branches (m, n) starting from node m is denoted with $\mathcal{B}_{(m, \cdot)}$ and a subset of all branches (m, n) ending at node n is denoted with $\mathcal{B}_{(\cdot, n)}$. Fig. 1 displays the structure of an example complex network in the EPANET tool. The dynamics of the WDS model is derived from a sequence of ordinary differential equations (ODEs) that describe the rate of change of the water level in storage units and has the following form:

$$\frac{dh_n}{dt} = \frac{1}{A_n} \left(\sum_{b \in \mathcal{B}_{(\cdot, n)}} q_b - \sum_{b \in \mathcal{B}_{(n, \cdot)}} q_b \right), \quad (1)$$

where $n \in \mathcal{N}_{\text{storage}}$ and $\mathcal{N}_{\text{storage}}$ is the set of storages in the WDS, A_n [m²] denotes the horizontal cross-section of the n th storage unit, t is the time, q_b [m³/s] represents the flow through branch b , whereas if it is described with pair (m, n) , $q_b > 0$ if water flows from m to n and $q_b < 0$ if water flows from n to m . The Hazen–Williams formula is used to determine the pressure difference between the nodes m and n bordering a pipe which constitutes a branch (m, n) indexed with b (Rossman et al., 2020):

$$p_n = p_m + \rho g \Delta h_{m,n} - \text{sgn}(q_b) \cdot \alpha \cdot \frac{L_b}{C_b^{1.852} \cdot d_b^{4.871}} \cdot |q_b|^{1.852}, \quad (2)$$

where p_m [Pa] and p_n [Pa] are the pressures at nodes m and n , respectively, ρ [kg/m³] is the water density, g [m/s²] is the acceleration of gravity, $\Delta h_{m,n}$ [m] is the difference in elevation between nodes m and n , L_b [m] is the pipe length, d_b [m] is the pipe inner diameter, C_b is the unitless Hazen–Williams roughness coefficient and the conversion coefficient α [m^{1.852}/m^{1.685}] is equal to 1.0453×10^5 . In this paper, for node n pressure p_n corresponds to the overpressure relative to the atmospheric pressure. The leakage flow at certain node n is modelled as (Van Zyl & Clayton, 2007):

$$q_{\text{loss},n} = A_{\text{leak},n} \sqrt{\frac{2}{\rho} p_n} \left[\frac{\text{m}^3}{\text{s}} \right], \quad (3)$$

where $A_{\text{leak},n}$ denotes the area of the leak surface at node n .

The setting of the PBV determines the desired pressure difference along it, so the pressure difference Δp_{PBV} across the PBV placed

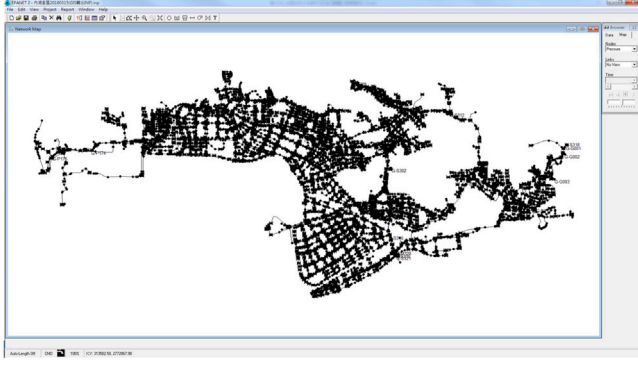


Fig. 1. Example of a complex water distribution network (Shiu, Chiang, & Chung, 2022).

between nodes m and n , $m < n$, is modelled as:

$$p_n = p_m - \text{sgn}(q) \cdot \Delta p_{PBV}, \quad \Delta p_{PBV} \geq 0. \quad (4)$$

The pressure difference Δp_{PDP} across the pressure-driven pump (PDP) placed between nodes m and n , $m < n$, is modelled as:

$$p_n = p_m + \Delta p_{PDP}. \quad (5)$$

If n is the storage output node placed at the bottom of the storage, the pressure at node n is:

$$p_n = \rho g h_n. \quad (6)$$

In the network, pressure-driven nodes (PDNs) are nodes in which the pressure at a particular time instant does not depend on the inputs setting or demands at that time — all nodes with water storage are pressure-driven nodes as well as all nodes in which the pressure is kept at a fixed value. Hence, if n is a non-storage pressure-driven node, the following holds:

$$p_n = p_{PDN}, \quad (7)$$

where p_{PDN} is the atmospheric overpressure of the pressure-driven node that is kept at a fixed value. In the case of a flow-driven pump (FDP), the flow through the branch b where the pump is located is defined as:

$$q_b = q_{FDP}, \quad (8)$$

where q_{FDP} is the flow through the flow-driven pump. Otherwise, the flow through the branch is determined by Eq. (2):

$$q_b = \text{sgn}(r_{m,n}) \cdot \left(\frac{|r_{m,n}| \cdot C_b^{1.852} \cdot d_b^{4.871}}{\alpha \cdot L_b} \right)^{\frac{1}{1.852}}, \quad (9)$$

where $r_{m,n} = p_m - p_n + \rho \cdot g \cdot \Delta h_{m,n}$. Since Eq. (9) has an infinite first derivative at point zero, its behaviour in the interval $r_{m,n} \in [-\varepsilon, +\varepsilon]$ is approximated by a linear function. The parameter ε is a small enough number introduced to ensure numerical stability. The pressure-driven demand $d_{\text{dem},n}$ at node n is modelled through the demand satisfaction ratio (DSR) (Muranho, Ferreira, Sousa, Gomes, & Marques, 2020):

$$d_{\text{dem},n} = D_{\text{dem},n} \cdot \text{DSR}_n, \quad (10)$$

$$\text{DSR}_n = \begin{cases} 1 & p_n \geq p_{\max} \\ \left(\frac{p_n - p_{\min}}{p_n - p_{\max}} \right)^\eta & p_{\min} < p_n < p_{\max} \\ 0 & p_n \leq p_{\min} \end{cases} \quad (11)$$

where $D_{\text{dem},n}$ is the high-pressure demand (HPD) at node n , p_n is the pressure at node n , p_{\min} is the pressure below which no water can be supplied, p_{\max} is the pressure necessary to fully satisfy the required demand $D_{\text{dem},n}$ and η is an exponent, usually with a value of 0.5 (Rossman et al., 2020).

The electrical power for the case of the flow-driven pump is calculated as:

$$S_{\text{FDP}} = \frac{\Delta p_{\text{FDP}} \cdot q_{\text{FDP}}}{\eta_{\text{FDP}}} \text{ [W]}, \quad (12)$$

where Δp_{FDP} is the pressure difference across a flow-driven pump and η_{FDP} is its electromechanical conversion efficiency. Furthermore, the electrical power for the case of the pressure-driven pump is calculated as:

$$S_{\text{PDP}} = \frac{\Delta p_{\text{PDP}} \cdot q_{\text{PDP}}}{\eta_{\text{PDP}}} \text{ [W]}, \quad (13)$$

where q_{PDP} is the flow through a pressure-driven pump and η_{PDP} is its electromechanical conversion efficiency.

The nonlinear state-space model of a WDS in general form is described as follows:

$$\dot{\mathbf{x}} = f_c(\mathbf{x}, \mathbf{u}, \mathbf{d}), \quad (14)$$

where the system states $\mathbf{x} \in \mathbb{R}^{n_x}$ are the water levels h_n in the WDS storages:

$$\mathbf{x} = [(h_n)_{n \in \mathcal{N}_{\text{storage}}}]^T. \quad (15)$$

The function $f_c : \mathbb{R}^{n_x} \times \mathbb{R}^{n_u} \times \mathbb{R}^{n_d} \rightarrow \mathbb{R}^{n_x}$ is a general nonlinear vector function and $\dot{\mathbf{x}}$ represents the time-derivative of \mathbf{x} .

The actuators in the WDS – pumps and valves – are assumed to be equipped with local controllers with the ability of continuous performance in regulating the required pressure or flow on them, in the space defined by physical constraints of the individual element, e.g. in the form of the nominal Q - H characteristics for a concrete pump. The WDS model thus includes also the flows or pressures that should be maintained on individual controllable system elements. Control commands provided from the central WDS controller for these individual local control circuits are in the form of their respective reference signals. For the presumed sampling time of the WDS system, the local controller behaviour can be approximated with a simple identity between the feasible reference value command and the specific flow or pressure that is being maintained on that reference value. Thus, although actually the reference value commands for specific controllable flows and pressures would be the control inputs of the WDS system (14), due to this presumed identity these controllable flows and pressures will be in the sequel considered as control input variables of the WDS system. Physical constraints of individual pumps and valves are used in the subsequent control problem formulation to assure feasibility of the issued commands.

The flows through the flow-driven pumps q_{FDP} , pressure differences across the pressure breaker valves, Δp_{PBV} , and pressure differences across the pressure-driven pumps, Δp_{PDP} , are thus the system control inputs $\mathbf{u} \in \mathbb{R}^{n_u}$:

$$\mathbf{u} = [(q_{\text{FDP},b})_{b \in \mathcal{B}_{\text{FDP}}}, (\Delta p_{\text{PBV},b})_{b \in \mathcal{B}_{\text{PBV}}}, (\Delta p_{\text{PDP},b})_{b \in \mathcal{B}_{\text{PDP}}}]^T, \quad (16)$$

where \mathcal{B}_{FDP} is the set of branches with flow-driven pumps, \mathcal{B}_{PBV} is the set of branches with pressure breaker valves and \mathcal{B}_{PDP} is the set of branches with pressure-driven pumps. Branches with the aforementioned elements contain only them; they have no pipe characteristics assigned and practically represent just segments between end-nodes of these physical elements. The sets \mathcal{B}_{FDP} , \mathcal{B}_{PBV} and \mathcal{B}_{PDP} consist of integers, representing integers of respective branches to which they are assigned.

The disturbance inputs in the system, denoted as $\mathbf{d} \in \mathbb{R}^{n_d}$, actually represent the high-pressure demands in various points of the network considered, $D_{\text{dem},n}$, as well as pressures in pressure-driven non-storage nodes (externally driven on a fixed pressure at a certain time instant):

$$\mathbf{d} = [(D_{\text{dem},n})_{n \in \mathcal{N}_{\text{HPD}}}, (p_n)_{n \in \mathcal{N}_{\text{PDN}}}]^T, \quad (17)$$

where \mathcal{N}_{HPD} is the set of WDS nodes with assigned demand and \mathcal{N}_{PDN} is the set of non-storage pressure-driven nodes in the network. Both sets comprise integers used to index individual nodes. It is worth noting

Table 1
Description of state-space model variables and parameters.

	Notation	Description	Units
States	$(h_n)_{n \in \mathcal{N}_{\text{storage}}}$	Water levels in the WDS storages	m
Inputs	$(q_{\text{FDP},b})_{b \in \mathcal{B}_{\text{FDP}}}$	(Reference) flows through the flow-driven pumps	m ³ /s
	$(\Delta p_{\text{PBV},b})_{b \in \mathcal{B}_{\text{PBV}}}$	(Reference) pressure differences across the pressure breaker valves	Pa
	$(\Delta p_{\text{PDP},b})_{b \in \mathcal{B}_{\text{PDP}}}$	(Reference) pressure differences across the pressure-driven pumps	Pa
Disturbances	$(D_{\text{dem},n})_{n \in \mathcal{N}_{\text{HFD}}}$	High-pressure demands	m ³ /s
	$(p_n)_{n \in \mathcal{N}_{\text{FDN}}}$	Pressures in pressure-driven non-storage nodes	Pa
Outputs	$(p_n)_{n \in \mathcal{N}_{\text{pressure}}}$	Pressures in specific nodes of interest in the network	Pa
	$(q_b)_{b \in \mathcal{B}_{\text{flow}}}$	Flows in specific branches of interest in the network	m ³ /s
	$(q_{\text{loss},n})_{n \in \mathcal{N}_{\text{loss}}}$	Losses occurring in specific nodes of the network	m ³ /s
	$(S_{\text{FDP},b})_{b \in \mathcal{B}_{\text{FDP}}}$	Flow-driven pump electrical power	W
	$(S_{\text{PDP},b})_{b \in \mathcal{B}_{\text{PDP}}}$	Pressure-driven pump electrical power	W
Parameters	$(A_n)_{n \in \mathcal{N}_{\text{storage}}}$	Horizontal cross-section of the storage	m ²
	ρ	Water density	kg/m ³
	g	Acceleration of gravity	m/s ²
	$\Delta h_{m,n}$	Difference in elevation between nodes m and n	m
	L_b	Length of the pipe represented with branch b of the network	m
	d_b	Inner diameter of the pipe represented with branch b of the network	m
	C_b	The pipe (branch b) Hazen-Williams roughness coefficient	–
	α	Conversion coefficient	$\frac{\text{s}^{1.852}}{\text{m}^{1.685}}$
	$A_{\text{leak},n}$	Area of the leak surface at node $n \in \mathcal{N}_{\text{loss}}$	m ²
	p_{min}	Pressure below which no water can be supplied	Pa
	p_{max}	Pressure necessary to fully satisfy the required demand $D_{\text{dem},n}$	Pa
	η	Exponent in the demand satisfaction ratio formula	–
	η_{FDP}	Electromechanical conversion efficiency of a flow-driven pump	–
	η_{PDP}	Electromechanical conversion efficiency of a pressure-driven pump	–

here that the demand in each node is potentially an aggregate of demands from multiple end-users of fresh water which are situated in the marginal part of the network that is not considered in the WDS model. Analogous note holds also for the loss assigned to the node. The decision of exclusion of some marginal parts of the network from consideration is not a consequence of inability to model them with the elaborated procedure, but rather a consequence of insufficient accuracy in predicting demands of individual end-users on a time resolution required for operating predictive control. That is why it is often beneficial to group more end-users in a single virtual demand point whose demand follows more closely a classical Gaussian random variable and is thus more easy to predict.

The system outputs $\mathbf{y} \in \mathbb{R}^y$ can be represented as a static function of state, controllable and disturbance inputs:

$$\mathbf{y} = g(\mathbf{x}, \mathbf{u}, \mathbf{d}), \quad (18)$$

where $g : \mathbb{R}^{n_x} \times \mathbb{R}^{n_u} \times \mathbb{R}^{n_d} \rightarrow \mathbb{R}^y$ is again a general nonlinear vector function. The system outputs considered include pressures, flows, and losses in specific segments of the network, and all pumps powers, as follows:

$$\mathbf{y} = \begin{bmatrix} (p_n)_{n \in \mathcal{N}_{\text{pressure}}} \\ (q_b)_{b \in \mathcal{B}_{\text{flow}}} \\ (q_{\text{loss},n})_{n \in \mathcal{N}_{\text{loss}}} \\ (S_{\text{FDP},b})_{b \in \mathcal{B}_{\text{FDP}}} \\ (S_{\text{PDP},b})_{b \in \mathcal{B}_{\text{PDP}}} \end{bmatrix}, \quad (19)$$

where $\mathcal{N}_{\text{pressure}}$ is the set of nodes in the network where pressures should be maintained within a certain range, $\mathcal{B}_{\text{flow}}$ is the set of branches in the network where flows should be maintained and $\mathcal{B}_{\text{loss}}$ is the set of network nodes where losses exist. The pressures $(p_n)_{n \in \mathcal{N}_{\text{pressure}}}$ can be expressed using the vector of system outputs as:

$$(p_n)_{n \in \mathcal{N}_{\text{pressure}}} = \mathbf{P}_n \cdot \mathbf{y}, \quad (20)$$

where \mathbf{P}_n represents the pressure selection matrix. For the sake of clarity, all variables of the WDS state space model and parameters are listed in Table 1 with the corresponding measurement units.

3. WDS optimization

The operational cost of the WDS during a specific time period consists of the combined costs associated with electrical energy consumed by the pumps and the volume of water lost through leaks. The primary objective in operating the WDS is to fulfil all demands at demand nodes with adequate pressures and flows maintained, while minimizing operational costs. For computer-based decision-making and optimization, the behaviour of a continuous-time WDS is represented through variables samples taken in discrete time instants. They are evenly distanced in time, and the corresponding sampling time is denoted with T . The values of time-dependent variables $\mathbf{x}, \mathbf{u}, \mathbf{d}$ or \mathbf{y} at a specific time kT that is an integer multiple of the sampling time, i.e. $k \in \mathbb{Z}$, are denoted with $\mathbf{x}_k, \mathbf{u}_k, \mathbf{d}_k$ and \mathbf{y}_k , respectively. Under the assumption of constant inputs \mathbf{u} and \mathbf{d} between the sampling instants, that is in time period

$$\mathcal{T}_k = [kT, (k+1)T), \quad (21)$$

the nonlinear continuous-time dynamics represented with f_c in (14) is transformed in the discrete-time form

$$\mathbf{x}_{k+1} = f_d(\mathbf{x}_k, \mathbf{u}_k, \mathbf{d}_k), \quad (22)$$

where $f_d : \mathbb{R}^{n_x} \times \mathbb{R}^{n_u} \times \mathbb{R}^{n_d} \rightarrow \mathbb{R}^{n_x}$.

The cost function for the considered WDS is defined as follows:

$$\mathcal{J} = \sum_{k=0}^{N-1} a_{e,k} E_k + a_w W_k, \quad (23)$$

where $a_{e,k}$ [$\frac{\text{EUR}}{\text{kWh}}$] is the price of electricity in the time period \mathcal{T}_k , E_k [kWh] is the electrical energy consumed by the pumps in \mathcal{T}_k , a_w [$\frac{\text{EUR}}{\text{m}^3}$] is the price for lost water for the utility, W_k [m³] is the volume of the lost water in \mathcal{T}_k and NT is the prediction horizon. The electrical energy consumed by both flow-driven and pressure-driven pumps in the time interval \mathcal{T}_k is determined as:

$$E_k = \frac{1}{3600 \cdot 1000} \left(\sum_{b \in \mathcal{B}_{\text{FDP}}} \int_{kT}^{(k+1)T} S_{\text{FDP},b}(t) dt + \sum_{b \in \mathcal{B}_{\text{PDP}}} \int_{kT}^{(k+1)T} S_{\text{PDP},b}(t) dt \right), \quad (24)$$

while the volume of lost water in \mathcal{T}_k is:

$$W_k = \sum_{n \in \mathcal{N}_{\text{loss}}} \int_{kT}^{(k+1)T} q_{\text{loss},n}(t) dt. \quad (25)$$

The integrals in Eqs. (24) and (25) are numerically solved, by applying the trapezoidal rule on the values at the sampling instants.

Since it is necessary to meet all pressure requirements, pressure constraints can be posed at any node of interest of the WDS as follows:

$$P_{\min,n} \leq p_{n,k} \leq P_{\max,n} \quad k = 0, \dots, N-1, \quad (26)$$

where $P_{\min,n}$ and $P_{\max,n}$ are the minimum and maximum allowed pressure at node $n \in \mathcal{N}_{\text{pressure}}$. Constraints are posed for branch $b \in \mathcal{B}_{\text{flow}}$ as follows:

$$Q_{\min,b} \leq q_{b,k} \leq Q_{\max,b} \quad k = 0, \dots, N-1, \quad (27)$$

where $Q_{\min,b}$ and $Q_{\max,b}$ are the minimum and maximum allowed flow through the branch b . Similarly, the constraints are posed also on the water heights in the n th storage tank along the prediction horizon:

$$H_{\min,n} \leq h_{n,k} \leq H_{\max,n} \quad k = 0, \dots, N-1, \quad (28)$$

where $H_{\min,n}$ and $H_{\max,n}$ are minimum and maximum allowed water levels in the storage tank $n \in \mathcal{N}_{\text{storage}}$, respectively. Constraints are also posed on the flows through flow-driven pumps, on the pressure differences across pressure breaker valves and on the pressure differences across pressure-driven pumps, as follows:

$$Q_{\text{FDP},\min,b} \leq q_{\text{FDP},b,k} \leq Q_{\text{FDP},\max,b} \quad b \in \mathcal{B}_{\text{FDP}}, \quad (29)$$

$$0 \leq \Delta p_{\text{PBV},b,k} \leq \Delta P_{\text{PBV},\max,b} \quad b \in \mathcal{B}_{\text{PBV}}, \quad (30)$$

$$\Delta P_{\text{PDP},\min,b} \leq \Delta p_{\text{PDP},b,k} \leq \Delta P_{\text{PDP},\max,b} \quad b \in \mathcal{B}_{\text{PDP}}, \quad (31)$$

where $k = 0, \dots, N-1$, $Q_{\text{FDP},\min,b}$ and $Q_{\text{FDP},\max,b}$ are the maximum and minimum allowed flows through the flow-driven pump in branch $b \in \mathcal{B}_{\text{FDP}}$, $\Delta P_{\text{PBV},\max,b}$ is the maximum allowed pressure difference across the PBV in branch $b \in \mathcal{B}_{\text{PBV}}$, $\Delta P_{\text{PDP},\min,b}$ and $\Delta P_{\text{PDP},\max,b}$ are the minimum and maximum allowed pressure differences across the pressure-driven pump in branch $b \in \mathcal{B}_{\text{PDP}}$, respectively.

The nonlinear optimization problem for day-ahead scheduling is posed here also with the initial state \mathbf{x}_0 used within the optimization variable, where the usual daily periodicity in operation is required to determine the best possible behaviour for a repeatable daily disturbance sequence $\mathbf{d}_0, \mathbf{d}_1, \dots, \mathbf{d}_{N-1}$, and this results in the constraint on repeatability of states

$$h_{n,0} = h_{n,N} \quad \forall n \in \mathcal{N}_{\text{storage}}. \quad (32)$$

The optimization problem is as follows:

$$\begin{aligned} & \min_{\mathbf{x}_0, \mathbf{u}_0, \mathbf{u}_1, \dots, \mathbf{u}_{N-1}} \mathcal{J} \\ & \text{subject to (22)–(32)}, \end{aligned} \quad (33)$$

where the optimization variable \mathbf{z} is defined as

$$\mathbf{z} = [\mathbf{x}_0^T \quad \mathbf{u}_0^T \quad \mathbf{u}_1^T \quad \dots \quad \mathbf{u}_{N-1}^T]^T. \quad (34)$$

As the general WDS model described in Section 2 is nonlinear, solving the optimization problem is performed iteratively by linearizing the model. This linearized representation can then be used to solve the problem for a small change in the initial conditions and control inputs, as a linear program (LP). Next, it is shown how the linear approximation of the WDS behaviour for small changes of inputs or states can be done, for a general WDS.

3.1. General network solving for sensitivity analysis at an operation point

In this research, the fourth order Runge–Kutta method (RK4) (Press, Teukolsky, Vetterling, & Flannery, 2007) is used to numerically solve Eq. (14) along the entire prediction horizon. EPANET was used to determine all pressures and flows in the network for given \mathbf{x}_k , \mathbf{u}_k and \mathbf{d}_k which are needed to evaluate the right-hand side of the differential Eq. (14) in the steps of Runge–Kutta method. This choice was made because of EPANET's capacity to quickly calculate the instantaneous pressures and flows throughout the entire network. The linearization of the different elements of this optimization problem was performed around the sequence of operating points determined with \mathbf{z}_0 , obtained by combining RK4 method of numerical integration and EPANET. In the context of WDS model, each operating point determined with \mathbf{z}_0 at the time point $t = kT$ is defined by fixed states $\mathbf{x}_{k,0}$ and control inputs $\mathbf{u}_{k,0}$ along with predicted disturbances $\mathbf{d}_{k,0}$ defined with (15)–(17). Along with $\mathbf{x}_{k,0}$, $\mathbf{u}_{k,0}$ and $\mathbf{d}_{k,0}$ all pressures, flows and losses in the network are determined for discrete times $k = 0, \dots, N-1$:

$$\begin{bmatrix} (p_{n,k,0})_{n \in \mathcal{N}} \\ (q_{b,k,0})_{b \in \mathcal{B}} \\ (q_{\text{loss},n,k,0})_{n \in \mathcal{N}_{\text{loss}}} \end{bmatrix} = f_{\text{OP}}(\mathbf{x}_{k,0}, \mathbf{u}_{k,0}, \mathbf{d}_{k,0}). \quad (35)$$

For each discrete time-step k the network sensitivity computation needs to be performed, which aims to assess how small changes in states, control inputs and disturbances of the network affect pressures, flows, losses and demands. In the following, to simplify the explanation the time index k in the variables is omitted. The states, i.e heights and changes to control and disturbance inputs for the entire network can be written as:

$$h_n = h_{n,0} + \Delta h_n \quad n \in \mathcal{N}_{\text{storage}}, \quad (36)$$

$$q_{\text{FDP},b} = q_{\text{FDP},b,0} + \Delta q_{\text{FDP},b} \quad b \in \mathcal{B}_{\text{FDP}}, \quad (37)$$

$$\Delta p_{\text{PBV},b} = \Delta p_{\text{PBV},b,0} + \Delta(\Delta p_{\text{PBV},b}) \quad b \in \mathcal{B}_{\text{PBV}}, \quad (38)$$

$$\Delta p_{\text{PDP},b} = \Delta p_{\text{PDP},b,0} + \Delta(\Delta p_{\text{PDP},b}) \quad b \in \mathcal{B}_{\text{PDP}}, \quad (39)$$

$$D_{\text{dem},n} = D_{\text{dem},n,0} + \Delta D_{\text{dem},n} \quad n \in \mathcal{N}_{\text{HPD}}, \quad (40)$$

where Δh_n , $\Delta q_{\text{FDP},b}$, $\Delta(\Delta p_{\text{PBV},b})$, $\Delta(\Delta p_{\text{PDP},b})$ and $\Delta D_{\text{dem},n}$ are small changes around the operating point. Changes of pressures, flows and power consumptions are introduced in the following manner:

$$p_n = p_{n,0} + \Delta p_n \quad n \in \mathcal{N}, \quad (41)$$

$$q_b = q_{b,0} + \Delta q_b \quad b \in \mathcal{B}, \quad (42)$$

$$q_{\text{loss},n} = q_{\text{loss},n,0} + \Delta q_{\text{loss},n} \quad n \in \mathcal{N}_{\text{loss}}, \quad (43)$$

$$S_{\text{FDP},b} = S_{\text{FDP},b,0} + \Delta S_{\text{FDP},b} \quad b \in \mathcal{B}_{\text{FDP}}, \quad (44)$$

$$S_{\text{PDP},b} = S_{\text{PDP},b,0} + \Delta S_{\text{PDP},b} \quad b \in \mathcal{B}_{\text{PDP}}. \quad (45)$$

In order to find relations between changes in (36)–(40) and (41)–(45), the following procedure is applied:

- The network is first by virtual cuts decomposed into paths where loops are eliminated, by eliminating branches with the highest resistance for a specific loop.
- Flow-driven pumps have infinity resistance while PDPs and PBVs have zero-resistance.
- Resistance of other branches is determined based on last term in Eq. (2).
- Virtual cuts are also introduced in paths that connect PDNs such that there is no connection between PDNs in the network through the retained branches.

The paths are virtually cut on branches with high resistance for numerical stability of subsequent linearization of the network since the flow change through these branches is least sensitive to changes of pressure in the respective branch end-points. The variables considered further in

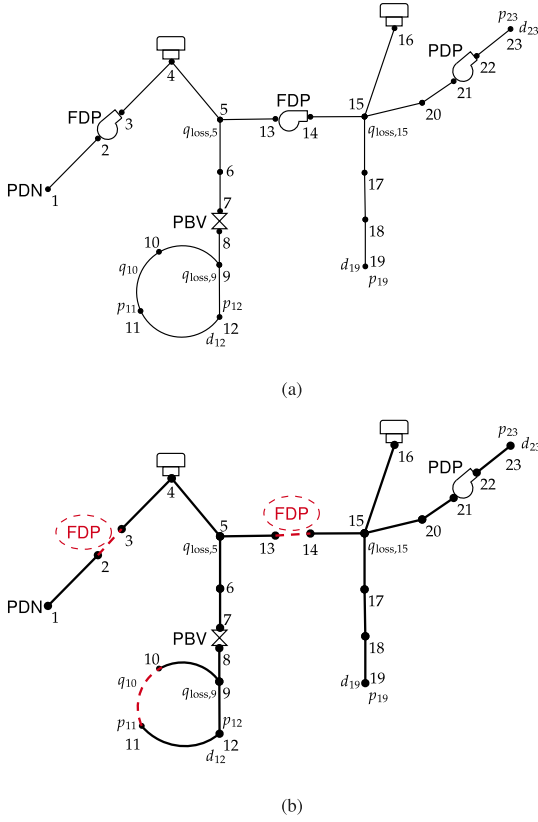


Fig. 2. (a) An example of a network where additional labels p , q , q_{loss} , and d indicate the nodes where it is necessary to maintain pressure, where it is necessary to maintain flow, where there are losses, and where demands are defined, respectively. (b) The network from Fig. 2(a) after introducing virtual cuts and thus obtaining cut paths for the subsequent sensitivity analysis.

the network are: pressures in PDNs, flows in remaining network paths after the virtual cuts are introduced (termed ‘other flows’) and flows through virtually cut branches (termed ‘connecting flows’). Let the set of branches exhibiting other flows and connecting flows be defined by B_{of} and B_{cf} , respectively.

Fig. 2(a) depicts a small network on which the introduced approach to network solving is illustrated. The network is decomposed into paths intersecting at the locations of the flow-driven pumps, specifically between nodes 2 and 3, and nodes 13 and 14. Since the network forms a loop delineated by nodes 9, 10, 11, and 12, it is necessary to cut the loop at the branch with the highest resistance, which is in this network for instance the branch between nodes 10 and 11. The network decomposed in this way is shown in Fig. 2(b). Appendix A contains all the sets defined so far for the network example shown in Fig. 2(a). In the following it will be assumed that the network is regular, which means that: (i) in the network there are no loops consisting of PDPs and/or PBVs only, and (ii) in the network there are no non-pressure-driven nodes in which meet only branches where flow is dictated by FDPs. The sensitivity analysis introduced here is applicable to any regular network.

Small changes in pressures, flows, and losses around the operating point are represented through linear relationships using small changes in state $\Delta \mathbf{x}$, control inputs $\Delta \mathbf{u}$, and demands $\Delta \mathbf{d}$. This is achieved by applying a first-order Taylor approximation of the model nonlinearities. The motivation for using Taylor series expansion is that it provides insight into how small changes in flow, pressure, and losses affect the system’s behaviour. The accuracy of linearization is maintained by limiting small changes in both states and control inputs, as explained in more detail in Section 4. Furthermore, small changes in pressures,

flows and losses are expressed in terms of matrices of coefficients $\mathbf{K}_{p,n}$, $\mathbf{K}_{q,b}$, $\mathbf{K}_{l,n}$ as follows:

$$\Delta p_n = \mathbf{K}_{p,n} \cdot \begin{bmatrix} \Delta \mathbf{x} \\ \Delta \mathbf{u} \\ \Delta \mathbf{d} \end{bmatrix} \quad n \in \mathcal{N}_{\text{pressure}}, \quad (46)$$

$$\Delta q_b = \mathbf{K}_{q,b} \cdot \begin{bmatrix} \Delta \mathbf{x} \\ \Delta \mathbf{u} \\ \Delta \mathbf{d} \end{bmatrix} \quad b \in B_{\text{flow}}, \quad (47)$$

$$\Delta q_{\text{loss},n} = \mathbf{K}_{l,n} \cdot \begin{bmatrix} \Delta \mathbf{x} \\ \Delta \mathbf{u} \\ \Delta \mathbf{d} \end{bmatrix} \quad n \in \mathcal{N}_{\text{loss}}. \quad (48)$$

Again, the small changes in states, control inputs and disturbances $\Delta \mathbf{x}$, $\Delta \mathbf{u}$ and $\Delta \mathbf{d}$, respectively, are small changes of variables in these vectors as defined with (15)–(17). The matrices of coefficients $\mathbf{K}_{p,n}$, $\mathbf{K}_{q,b}$ and $\mathbf{K}_{l,n}$ in expressions (46)–(48) are obtained as follows in Section 3.2.

3.2. Determining partial derivatives of WDS using virtual cuts

First, let S_{path} be the set of virtual cut paths of the network. Each virtual cut path contains exactly one pressure-driven node. Starting from that node, the pressure dependencies of other nodes are used in a chain procedure by applying (6) for the storage output node, (7) for PDN, (2) for pipes, (4) for PBV and (5) for PDP. If node n is either a storage output node or a pressure-driven node, expressions (6) and (7) must be respectively utilized as follows:

$$\frac{\partial p_n}{\partial(\mathbf{x}, \mathbf{u}, \mathbf{d})} = \rho g \cdot \frac{\partial h_n}{\partial(\mathbf{x}, \mathbf{u}, \mathbf{d})}, \quad (49)$$

$$\frac{\partial p_n}{\partial(\mathbf{x}, \mathbf{u}, \mathbf{d})} = \frac{\partial p_{\text{PDN}}}{\partial(\mathbf{x}, \mathbf{u}, \mathbf{d})}. \quad (50)$$

The partial derivative in Eq. (49) is always zero, except when it corresponds to an element from \mathbf{x} , which exactly represents that storage and in that case the derivative equals 1. Analogously, the partial derivative in Eq. (50) is zero unless it corresponds to an element from \mathbf{d} that specifically represents that pressure-driven node and in that case the derivative equals 1. The small change in pressure at node n , denoted as Δp_n , can be expressed as:

$$\Delta p_n = \sum_{j=1}^{n_x} \frac{\partial p_n}{\partial x_j} \Delta x_j + \sum_{j=1}^{n_u} \frac{\partial p_n}{\partial u_j} \Delta u_j + \sum_{j=1}^{n_d} \frac{\partial p_n}{\partial d_j} \Delta d_j, \quad (51)$$

and the same analogously holds for remaining changes of flows as introduced in (42) and (43). The partial derivative of expression (2) with respect to all system states, control inputs, and disturbances for a pipe is found as:

$$\frac{\partial p_n}{\partial(\mathbf{x}, \mathbf{u}, \mathbf{d})} = \frac{\partial p_m}{\partial(\mathbf{x}, \mathbf{u}, \mathbf{d})} - \frac{df(q_b)}{dq_b} \cdot \frac{\partial q_b}{\partial(\mathbf{x}, \mathbf{u}, \mathbf{d})}, \quad (52)$$

where b is the branch between nodes m and n and $f(q_b)$ represents the function of dependence of pressure with respect to flow, that is the right-hand side of Eq. (2). All flows q_b through branches that remain in the specific cut paths are grouped into the vector \mathbf{q}_{of} . If a PBV is positioned between nodes m and n , the necessary partial derivatives are computed from expression (4):

$$\frac{\partial p_n}{\partial(\mathbf{x}, \mathbf{u}, \mathbf{d})} = \frac{\partial p_m}{\partial(\mathbf{x}, \mathbf{u}, \mathbf{d})} + \frac{\partial \Delta p_{\text{PBV}}}{\partial(\mathbf{x}, \mathbf{u}, \mathbf{d})}. \quad (53)$$

The last term in Eq. (53) is always zero, except when it corresponds to an element from \mathbf{u} , which exactly represents that PBV. If a PDP is present between nodes m and n , expression (5) is employed:

$$\frac{\partial p_n}{\partial(\mathbf{x}, \mathbf{u}, \mathbf{d})} = \frac{\partial p_m}{\partial(\mathbf{x}, \mathbf{u}, \mathbf{d})} + \frac{\partial \Delta p_{\text{PDP}}}{\partial(\mathbf{x}, \mathbf{u}, \mathbf{d})}. \quad (54)$$

Again, the last term in Eq. (54) is always zero, except when it corresponds to an element from \mathbf{u} , which exactly represents that PDP.

Finally, using (51), small changes in pressures of all nodes $n \in \mathcal{N}$ through the small changes in all other flows, pressure differences across PBVs, pressure differences across PDPs, water levels in storages and

pressures of PDNs can be written as:

$$\begin{aligned} \Delta \mathbf{p} = & \mathbf{M}_{\text{pressure},1} \cdot \Delta \mathbf{p} + \mathbf{M}_{\text{pressure},2} \cdot \Delta \mathbf{q}_{\text{of}} + \\ & \mathbf{M}_{\text{pressure},3} \cdot \Delta(\Delta \mathbf{p}_{\text{PBV}}) + \mathbf{M}_{\text{pressure},4} \cdot \Delta(\Delta \mathbf{p}_{\text{PDP}}) + \\ & \mathbf{M}_{\text{pressure},5} \cdot \Delta \mathbf{h} + \mathbf{M}_{\text{pressure},6} \cdot \Delta \mathbf{p}_{\text{PDN}}, \end{aligned} \quad (55)$$

where $\mathbf{M}_{\text{pressure},1}$ to $\mathbf{M}_{\text{pressure},6}$ are matrices of derivatives for all virtual cut paths obtained by merging expressions (49), (50), (52)–(54) in (51).

Next, it is necessary to determine the expressions for small changes in connecting flows Δq_{cf} . Using expressions (8) and (9), the partial derivatives are obtained depending on whether the branch is flow-driven pump or pipe, respectively:

$$\frac{\partial q_{\text{cf}}}{\partial(\mathbf{x}, \mathbf{u}, \mathbf{d})} = \frac{\partial q_{\text{FDP}}}{\partial(\mathbf{x}, \mathbf{u}, \mathbf{d})}, \quad (56)$$

$$\frac{\partial q_{\text{cf}}}{\partial(\mathbf{x}, \mathbf{u}, \mathbf{d})} = \frac{df_{\text{cf}}(p_m, p_n)}{dp_m} \cdot \frac{\partial p_m}{\partial(\mathbf{x}, \mathbf{u}, \mathbf{d})} + \frac{df_{\text{cf}}(p_m, p_n)}{dp_n} \cdot \frac{\partial p_n}{\partial(\mathbf{x}, \mathbf{u}, \mathbf{d})}, \quad (57)$$

where $f_{\text{cf}}(p_m, p_n)$ represents the function in dependence of pressures p_m and p_n , that is the right-hand side of Eq. (9). Analogous to pressures, expressions for small changes in connecting flows are obtained as a linear function of small changes in flow through the flow-driven pumps and small changes in pressures.

$$\Delta \mathbf{q}_{\text{cf}} = \mathbf{M}_{\text{cf},1} \cdot \Delta \mathbf{q}_{\text{FDP}} + \mathbf{M}_{\text{cf},2} \cdot \Delta \mathbf{p}, \quad (58)$$

where $\mathbf{M}_{\text{cf},1}$ and $\mathbf{M}_{\text{cf},2}$ are matrices of derivatives for all virtually cut connections between the retained paths that employ partial derivatives obtained with (56) and (57) and merged into a Taylor series expansion for connecting flows analogous to relation (51). The third part of network sensitivity analysis is to determine the small change of losses using partial derivative of the expression (3):

$$\frac{\partial q_{\text{loss}}}{\partial(\mathbf{x}, \mathbf{u}, \mathbf{d})} = \frac{dq_{\text{loss}}(p_n)}{dp_n} \cdot \frac{\partial p_n}{\partial(\mathbf{x}, \mathbf{u}, \mathbf{d})}. \quad (59)$$

The small change of losses can be expressed as:

$$\Delta \mathbf{q}_{\text{loss}} = \mathbf{M}_{\text{loss}} \cdot \Delta \mathbf{p}, \quad (60)$$

where \mathbf{M}_{loss} is the matrix of derivatives obtained from (59). The same procedure applies to demands, specifically to relations (10) and (11):

$$\begin{aligned} \frac{\partial d_{\text{dem},n}}{\partial(\mathbf{x}, \mathbf{u}, \mathbf{d})} = & \frac{dd_{\text{dem},n}(p_n, D_{\text{dem},n})}{dp_n} \cdot \frac{\partial p_n}{\partial(\mathbf{x}, \mathbf{u}, \mathbf{d})} + \\ & \frac{dd_{\text{dem},n}(p_n, D_{\text{dem},n})}{dD_{\text{dem},n}} \cdot \frac{\partial D_{\text{dem},n}}{\partial(\mathbf{x}, \mathbf{u}, \mathbf{d})}. \end{aligned} \quad (61)$$

Moreover, the matrix equation of small changes in all demands through the small changes in pressures and high-pressure demands is as follows:

$$\Delta \mathbf{d}_{\text{dem}} = \mathbf{M}_{\text{dem},1} \cdot \Delta \mathbf{p} + \mathbf{M}_{\text{dem},2} \cdot \Delta \mathbf{D}_{\text{dem}}, \quad (62)$$

where $\mathbf{M}_{\text{dem},1}$ and $\mathbf{M}_{\text{dem},2}$ are matrices of derivatives obtained from (61).

From the network structure, a flow conservation equation is written for each node except pressure-driven nodes, i.e. $n \in \{\mathcal{N} \setminus (\mathcal{N}_{\text{PDN}} \cup \mathcal{N}_{\text{storage}})\}$:

$$\sum_{b \in \mathcal{B}(n)} q_b = \sum_{b \in \mathcal{B}(n,-)} q_b \quad n \in \{\mathcal{N} \setminus (\mathcal{N}_{\text{PDN}} \cup \mathcal{N}_{\text{storage}})\}. \quad (63)$$

For every node except the pressure-driven node in every retained path one can assign a one-to-one relation with a branch preceding this node when coming to it from the pressure-driven node. Since every retained path has exactly one pressure-driven node, this means that the overall number of other flows is exactly $|\mathcal{N}| - |\mathcal{N}_{\text{PDN}} \cup \mathcal{N}_{\text{storage}}|$. Relation (63) holds exactly that same number of equations with other flows which means that a regular linear system of equations arises with respect to other flows and it allows to express them explicitly with respect to connecting flows, losses and demands, as follows:

$$\Delta \mathbf{q}_{\text{of}} = \mathbf{M}_{\text{of},1} \cdot \Delta \mathbf{q}_{\text{cf}} + \mathbf{M}_{\text{of},2} \cdot \Delta \mathbf{q}_{\text{loss}} + \mathbf{M}_{\text{of},3} \cdot \Delta \mathbf{d}_{\text{dem}}. \quad (64)$$

Eq. (55) represents $|\mathcal{N}|$ equations for changes of pressures in $|\mathcal{N}|$ nodes. Quantities in it which are not part of $\Delta \mathbf{x}$, $\Delta \mathbf{u}$ and $\Delta \mathbf{d}$ can be

expressed linearly with $\Delta \mathbf{p}$ and $\Delta \mathbf{x}$, $\Delta \mathbf{u}$, $\Delta \mathbf{d}$ by employing (58), (60), (62) and (64). This finally leads to the system of $|\mathcal{N}|$ linear equations with $|\mathcal{N}|$ $\Delta \mathbf{p}$ unknowns which can be solved thus leading to explicit expression of $\Delta \mathbf{p}$ with respect to $\Delta \mathbf{x}$, $\Delta \mathbf{u}$, $\Delta \mathbf{d}$, as follows:

$$\Delta \mathbf{p} = \mathbf{W}_{\text{pressure},x} \cdot \Delta \mathbf{x} + \mathbf{W}_{\text{pressure},u} \cdot \Delta \mathbf{u} + \mathbf{W}_{\text{pressure},d} \cdot \Delta \mathbf{d}. \quad (65)$$

Now with having $\Delta \mathbf{p}$ explicitly expressed with $\Delta \mathbf{x}$, $\Delta \mathbf{u}$ and $\Delta \mathbf{d}$, the remaining network quantities on the left-hand sides of Eqs. (58), (60), (62) and (64) can as well be expressed explicitly with respect to $\Delta \mathbf{x}$, $\Delta \mathbf{u}$ and $\Delta \mathbf{d}$, as follows:

$$\Delta \mathbf{q}_{\text{cf}} = \mathbf{W}_{\text{cf},x} \cdot \Delta \mathbf{x} + \mathbf{W}_{\text{cf},u} \cdot \Delta \mathbf{u} + \mathbf{W}_{\text{cf},d} \cdot \Delta \mathbf{d}, \quad (66)$$

$$\Delta \mathbf{q}_{\text{loss}} = \mathbf{W}_{\text{loss},x} \cdot \Delta \mathbf{x} + \mathbf{W}_{\text{loss},u} \cdot \Delta \mathbf{u} + \mathbf{W}_{\text{loss},d} \cdot \Delta \mathbf{d}, \quad (67)$$

$$\Delta \mathbf{d}_{\text{dem}} = \mathbf{W}_{\text{dem},x} \cdot \Delta \mathbf{x} + \mathbf{W}_{\text{dem},u} \cdot \Delta \mathbf{u} + \mathbf{W}_{\text{dem},d} \cdot \Delta \mathbf{d}, \quad (68)$$

$$\Delta \mathbf{q}_{\text{of}} = \mathbf{W}_{\text{of},x} \cdot \Delta \mathbf{x} + \mathbf{W}_{\text{of},u} \cdot \Delta \mathbf{u} + \mathbf{W}_{\text{of},d} \cdot \Delta \mathbf{d}. \quad (69)$$

Relation (46) directly corresponds to (65), relation (47) is obtained by merging (66) and (69), while (48) is exactly represented by (67). The elaborated procedure allows to analytically assess small changes in all pressures, flows, demands and losses in the network with respect to small changes of water heights in storages, small changes of control commands and small changes of high-pressure demands and pressures in non-storage pressure-driven nodes. It is universal for a regular WDS of an arbitrary structure and thus it enables to create a universal code for computing the network sensitivity, opening way for a universal code for sequential linear programming for WDS optimization which is described next.

4. Sequential linear program for WDS optimization

The methodology developed is targeted to improve the initial operation plan of the WDS given with:

$$\mathbf{z}_0 = \begin{bmatrix} \mathbf{x}_{0,0}^T & \mathbf{u}_{0,0}^T & \mathbf{u}_{1,0}^T & \cdots & \mathbf{u}_{N-1,0}^T \end{bmatrix}^T. \quad (70)$$

For these initial values the system model can be used in a system simulation set-up, relied on numerical integration procedures, to determine the response along the entire prediction horizon, i.e. the sequence of states along the prediction horizon $(\mathbf{x}_{0,0}, \mathbf{x}_{1,0}, \mathbf{x}_{2,0}, \dots, \mathbf{x}_{N-1,0}, \mathbf{x}_{N,0})$. From now on, small disturbance changes $\Delta \mathbf{d}$ will not be taken into account, as the demands are considered constant once they are predicted with a certain demand prediction algorithm and also an analogous claim holds for the pressures in non-storage pressure-driven nodes. From (1) and (47) for sufficiently small changes for each interval $[kT, (k+1)T)$ the following holds:

$$\frac{d\Delta \mathbf{x}(t)}{dt} = \mathbf{K}_{x,k} \Delta \mathbf{x}(t) + \mathbf{K}_{u,k} \Delta \mathbf{u}(t), \quad (71)$$

where $t \in \mathcal{T}_k$, $\mathbf{K}_{x,k} \in \mathbb{R}^{n_x \times n_x}$ and $\mathbf{K}_{u,k} \in \mathbb{R}^{n_x \times n_u}$ are corresponding matrices of derivatives.

After the discretization of Eq. (71) with the Zero-Order Hold (ZOH) method, the expression of the dependence of a small change in state, $\Delta \mathbf{x}$, namely, a small change in the water levels in the storages at time instant k , is obtained:

$$\Delta \mathbf{x}_{k+1} = \alpha_k \Delta \mathbf{x}_k + \beta_k \Delta \mathbf{u}_k, \quad (72)$$

where α_k and β_k are, respectively

$$\alpha_k = e^{\mathbf{K}_{x,k} T}, \quad (73)$$

$$\beta_k = (\mathbf{K}_{x,k})^{-1} \cdot (\alpha_k - \mathbf{I}) \cdot \mathbf{K}_{u,k}. \quad (74)$$

Now also all changes of states along the prediction horizon for $k = 0, 1, \dots, N$ can be expressed with respect to the change of the initial state $\Delta \mathbf{x}_0$ and the changes of the control input $\Delta \mathbf{u}_k$, $k = 0, 1, \dots, N-1$, as follows (Vařak & Novak, 2019):

$$\Delta \mathbf{X} = \mathbf{A} \Delta \mathbf{x}_0 + \mathbf{B} \Delta \mathbf{U}, \quad (75)$$

$$\mathbf{A} = \begin{bmatrix} \mathbf{I} \\ \alpha_0 \\ \alpha_0 \alpha_1 \\ \vdots \\ \prod_{i=0}^{N-1} \alpha_i \end{bmatrix}, \quad (76)$$

$$\mathbf{B} = \begin{bmatrix} \mathbf{0} & \mathbf{0} & \cdots & \mathbf{0} \\ \beta_0 & \mathbf{0} & \cdots & \mathbf{0} \\ \alpha_1 \beta_0 & \beta_1 & \cdots & \mathbf{0} \\ \vdots & \vdots & \cdots & \vdots \\ \left(\prod_{i=1}^{N-1} \alpha_i \right) \beta_0 & \left(\prod_{i=2}^{N-1} \alpha_i \right) \beta_1 & \cdots & \beta_{N-1} \end{bmatrix}, \quad (77)$$

with changes of states and control inputs defined as:

$$\Delta \mathbf{X} = [\Delta \mathbf{x}_0^T \quad \Delta \mathbf{x}_1^T \quad \cdots \quad \Delta \mathbf{x}_N^T]^T, \quad (78)$$

$$\Delta \mathbf{U} = [\Delta \mathbf{u}_0^T \quad \Delta \mathbf{u}_1^T \quad \cdots \quad \Delta \mathbf{u}_{N-1}^T]^T. \quad (79)$$

Furthermore, the changes of outputs $\Delta \mathbf{y}$ defined with Eq. (19) along the prediction horizon can also be expressed with respect to $\Delta \mathbf{x}_0$ and $\Delta \mathbf{U}$. Combining the coefficients from (46)–(48) yields the matrices \mathbf{C} and \mathbf{D} with respect to $\Delta \mathbf{X}$ and $\Delta \mathbf{U}$

$$\Delta \mathbf{Y} = \mathbf{C} \Delta \mathbf{X} + \mathbf{D} \Delta \mathbf{U}. \quad (80)$$

Substituting (75) into (80) yields the desired expression

$$\Delta \mathbf{Y} = \mathbf{C} \mathbf{A} \Delta \mathbf{x}_0 + (\mathbf{C} \mathbf{B} + \mathbf{D}) \Delta \mathbf{U}. \quad (81)$$

In order to obtain the formulation of a Linear Program (LP) for optimizing $\Delta \mathbf{x}_0$ and $\Delta \mathbf{U}$, it is necessary first to derive equations for E_k and W_k that depend on a small change in the initial state $\Delta \mathbf{x}_0$ and a small change in the control inputs $\Delta \mathbf{U}$, utilizing Eqs. (12), (13), (24), (25) and (81):

$$E_k = \frac{1}{2} \Delta \mathbf{z}^T \mathbf{F}_{E,k} \Delta \mathbf{z} + \mathbf{G}_{E,k} \Delta \mathbf{z} + E_{k,0}, \quad (82)$$

$$W_k = \mathbf{H}_{\text{loss},k} \Delta \mathbf{z} + W_{k,0}, \quad (83)$$

where $\mathbf{F}_{E,k} \in \mathbb{R}^{(n_x + N \cdot n_u) \times (n_x + N \cdot n_u)}$, $\mathbf{G}_{E,k} \in \mathbb{R}^{1 \times (n_x + N \cdot n_u)}$, $E_{k,0} \in \mathbb{R}$, $\mathbf{H}_{\text{loss},k} \in \mathbb{R}^{1 \times (n_x + N \cdot n_u)}$, $W_{k,0} \in \mathbb{R}$, $k = 0, 1, \dots, N-1$ and the small change of the optimization variable $\Delta \mathbf{z}$ is defined as

$$\Delta \mathbf{z} = [\Delta \mathbf{x}_0^T \quad \Delta \mathbf{U}^T]^T. \quad (84)$$

The cost function \mathcal{J} described with Eq. (23) can now be expressed with respect to the change of the optimization variable $\Delta \mathbf{z}$

$$\mathcal{J} = \frac{1}{2} \Delta \mathbf{z}^T \mathbf{R} \Delta \mathbf{z} + \mathbf{W} \Delta \mathbf{z} + \mathcal{J}_0, \quad (85)$$

where \mathbf{R} , \mathbf{W} and \mathcal{J}_0 are respectively:

$$\mathbf{R} = \sum_{k=0}^{N-1} a_{e,k} \mathbf{F}_{E,k}, \quad (86)$$

$$\mathbf{W} = \sum_{k=0}^{N-1} a_{e,k} \mathbf{G}_{E,k} + a_w \mathbf{H}_{\text{loss},k}, \quad (87)$$

$$\mathcal{J}_0 = \sum_{k=0}^{N-1} a_{e,k} E_{k,0} + a_w W_{k,0}. \quad (88)$$

Since there is no guarantee that the matrix \mathbf{R} is positive semidefinite, additional linearization around $\Delta \mathbf{z} = 0$ approximates the cost function \mathcal{J} so that the first term in (85) approaches zero, resulting in the following expression:

$$\mathcal{J} = \mathbf{W} \Delta \mathbf{z} + \mathcal{J}_0. \quad (89)$$

Furthermore, the constraints for the pressure (26) can be expressed by merging expressions (20), (41) and (81):

$$P_{\min,n} \leq p_{n,k,0} + \mathbf{P}_{n,k} \cdot ((\mathbf{C} \mathbf{A}) \cdot \Delta \mathbf{x}_0 + (\mathbf{C} \mathbf{B} + \mathbf{D}) \cdot \Delta \mathbf{U}) \leq P_{\max,n}, \quad (90)$$

where $\mathbf{P}_{n,k}$ is the selection matrix that extracts pressures from the vector of small output changes $\Delta \mathbf{Y}$ at each time instant k . Similarly, the constraints (27)–(31) can be expressed using the same procedure. Additionally, limiting small changes in states and control inputs is necessary to ensure the accuracy of linearization

$$-\Delta \mathbf{X}_{\min} \leq \Delta \mathbf{x}_k \leq \Delta \mathbf{X}_{\max}, \quad (91)$$

$$-\Delta \mathbf{U}_{\min} \leq \Delta \mathbf{u}_k \leq \Delta \mathbf{U}_{\max}, \quad (92)$$

where $\Delta \mathbf{X}_{\min}$ and $\Delta \mathbf{X}_{\max}$ are the vectors of the minimum and maximum allowed small changes in state, that is small changes in the water column height in the n th storage tank ($\Delta h_{n,k})_{n \in \mathcal{N}_{\text{storage}}}$, while $\Delta \mathbf{U}_{\min}$ and $\Delta \mathbf{U}_{\max}$ are the vectors of the minimum and maximum allowed small changes in control inputs ($\Delta(q_{\text{FDP},b,k})_{b \in \mathcal{B}_{\text{FDP}}}$, $\Delta(p_{\text{PBV},b,k})_{b \in \mathcal{B}_{\text{PBV}}}$ and $\Delta(p_{\text{PDP},b,k})_{b \in \mathcal{B}_{\text{PDP}}}$). The limits of small changes were selected to ensure that, during a series of simulations with complex network configurations, the solution remained feasible in all iterations. This indicates that the changes in the linearized model are small enough to closely follow the nonlinear model with high accuracy. The LP for a general WDS is derived by integrating all the previously described constraints. It can be expressed as follows:

$$\min_{\Delta \mathbf{z}} \mathcal{J} = \min_{\Delta \mathbf{z}} (\mathbf{W} \Delta \mathbf{z} + \mathcal{J}_0) \quad (93)$$

subject to:

$$\mathbf{A}_{\text{ineq}} \Delta \mathbf{z} \leq \mathbf{b}_{\text{ineq}}, \quad (94)$$

$$\mathbf{A}_{\text{eq}} \Delta \mathbf{z} = \mathbf{b}_{\text{eq}}. \quad (95)$$

The LP can be solved using one of the linear programming solvers, leading to locally optimal changes

$$\Delta \mathbf{z}_0^* = [(\Delta \mathbf{x}_0^*)^T \quad (\Delta \mathbf{u}_0^*)^T \quad (\Delta \mathbf{u}_1^*)^T \quad \cdots \quad (\Delta \mathbf{u}_{N-1}^*)^T]^T, \quad (96)$$

and finally, the improved optimization variable is obtained as

$$\mathbf{z}_1 = \mathbf{z}_0 + \Delta \mathbf{z}_0^*. \quad (97)$$

The optimization variable \mathbf{z}_1 is used as the initial point for the next iteration of the optimization in the SLP procedure. In the i th iteration of the SLP ($i = 1, 2, \dots$) the optimization variable \mathbf{z}_i is obtained

$$\mathbf{z}_i = \mathbf{z}_{i-1} + \Delta \mathbf{z}_{i-1}^*. \quad (98)$$

The sequence of SLP iterations can be stopped once the decrease in the optimal cost falls below a certain threshold for several iterations, or once the time allowed for computation has elapsed. The solution obtained in the last iteration step \mathcal{I}_{\max} , $\mathbf{z}_{\mathcal{I}_{\max}}$ is the improvement, potentially a substantial one, compared to the initial plan of running the system represented with \mathbf{z}_0 .

5. Case studies and results

A toy-example and a WDS segment of a city in Spain are processed in MATLAB with the code for optimization that just uses a specific description file in a universal format to accommodate to a specific WDS configuration. The algorithm is universal and applicable to regular networks of arbitrary structure. The sampling time (T) of 15 min was utilized. In this research, the parameter ε introduced in Section 2 is 20 Pa, and the solution remained feasible in each iteration, despite using very complex network configurations. In the following cases the price of electricity from including 07:00 to excluding 21:00 is 1 EUR/kWh, and at other times it is 0.2 EUR/kWh. Cost of lost water for utility company is set at 2 EUR/m³ throughout the day.

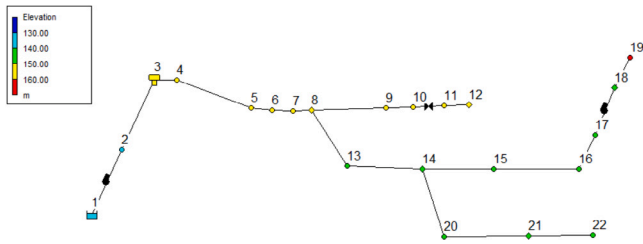


Fig. 3. WDS structure of the toy-example.

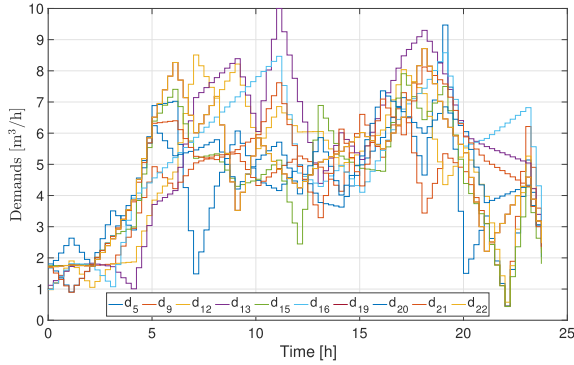


Fig. 4. High-pressure demands for the 9 supply nodes of the considered WDS, for the whole day.

5.1. Baseline operation of the toy-example case study

The considered WDS consists of 1 storage tank, 1 valve, 2 pumps, 21 branches and 22 nodes, and is structured as provided in Fig. 3. Demands are present in nodes denoted with the following indices: 5, 9, 12, 13, 15, 16, 19, 20, 21 and 22. Losses are assumed to occur in nodes: 8, 12, 14, 18 and 21. High-pressure demand profiles for the considered 10 supply nodes are provided in Fig. 4. The dimensions of all states, control inputs, and disturbances for the toy-example case study are presented in Table B.5, located in the Appendix B. All other parameters of the network from Table 1 are directly retrieved from the EPANET file. Hysteresis control was used as the baseline operation. With hysteresis control, the pump turns on if the water level in the tank falls below 17.5 m, and turns off if the water level rises above 22 m. The pump on and off levels are determined through simulation to ensure that the pressure at the end-points does not drop below the minimum allowed pressure, which is set to 1 bar (over the atmospheric pressure), in order to meet all the defined constraints on pressures with this control method. In hysteresis control, the settings of the PBV and the PDP are assumed to remain constant throughout the day. The simulation was repeated for several consecutive days, employing a repeating disturbance sequence until a steady-state diurnal harmonic behaviour was achieved. This was done to ensure a valid comparison with the SLP.

5.2. SLP operation of the toy-example case study

The optimization procedure, starting with the response of the baseline operation, yields the response of the storage level which is compared with the baseline control in Fig. 5. The input flow profile after application of the SLP procedure and the input flow profile obtained by baseline control are compared in Fig. 6. The optimal operation profiles of the PBV and the PDP are shown in Figs. 7 and 8. Pressures relative to the atmospheric pressure at the end-points marked with 12, 19 and 22 after application of the SLP procedure and during baseline control are shown in Fig. 9. Total cost of daily operation of the WDS through

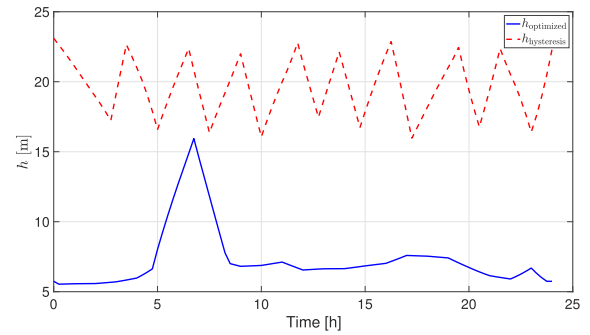


Fig. 5. Comparison of height profiles in the tank obtained using SLP and baseline control.

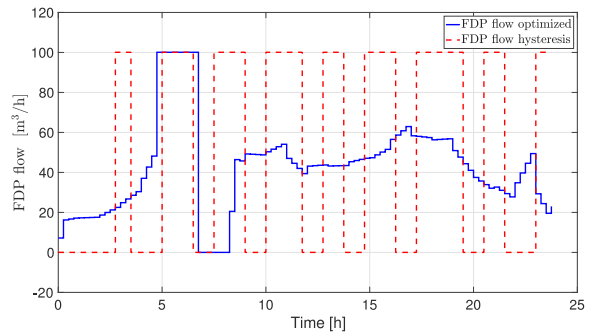


Fig. 6. Baseline and computed optimal FDP flow.

Table 2

Daily cost comparison for the toy-example.

	Overall cost for lost water [EUR]	Overall cost for electricity [EUR]	Total cost [EUR]
Baseline	204.60	133.78	338.38
SLP	160.59	78.56	239.15

iterations of the optimization procedure is shown in Fig. 10. The cost value at iteration zero represents the cost associated with the baseline operation. Comparison of costs due to water leakage and electricity as well as total costs comparison are shown in Table 2. The relative total cost savings using the SLP procedure compared to hysteresis control is 29.33%. The obtained responses provide a suggestion for pump operation to achieve maximum flow during periods of lower electricity prices but without overcharging the storage to evade high pressures and thus overly high losses. The optimal suggestions for the PDP and PBV involve minimizing pressure to reduce losses while ensuring that all requirements are met, such as maintaining overpressure greater or equal to 1 bar. The procedure was performed on an ARM-based Apple M1 SoC with 8 CPU and 8 GPU cores, while the RAM size is 8 GB. Maximum CPU clock rate is 3.2 GHz. MATLAB, in which the program is executed, is also ARM-based. The execution time for the whole optimization procedure including all the iterations shown as well as generating the model structure in MATLAB from the description file, is 51.7 s.

5.3. Baseline operation on WDS segment of a city in Spain

The considered WDS in the second case study consists of 10 storage tanks, 8 FDPs, 1 PDP, 8 PBVs, 7380 branches and 6992 nodes. Demands are specified across 631 nodes, with the distribution of the 10 demand examples from Fig. 4 among these nodes. Losses are assumed to occur in 728 nodes. The surface areas of leaks punctures are proportional to the variance of the diameters of all pipes that meet at node $n \in \mathcal{N}_{\text{loss}}$:

$$A_{\text{leak},n} = k_{\text{loss}} \cdot \text{var}(d_b) \quad b \in \mathcal{B}_{(n,\cdot)} \cup \mathcal{B}_{(\cdot,n)}, \quad (99)$$

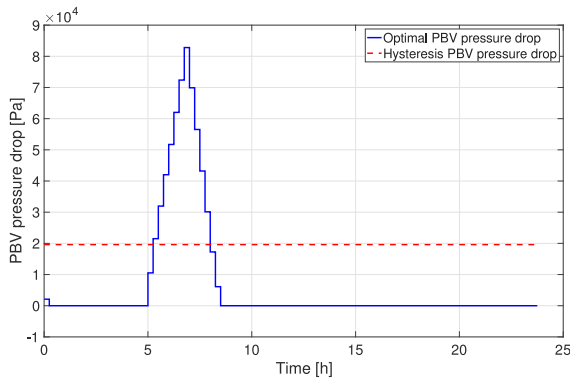


Fig. 7. Baseline and optimal PBV pressure drop profiles.

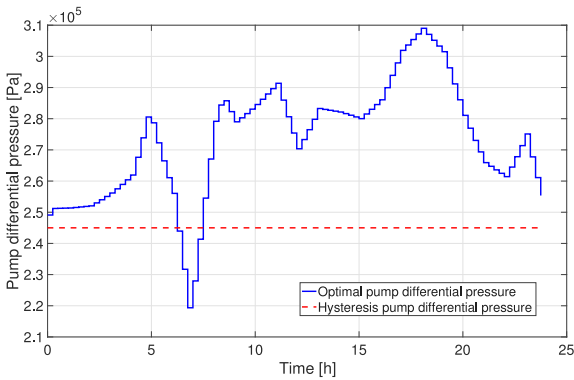


Fig. 8. Baseline and optimal pump difference pressure profiles.

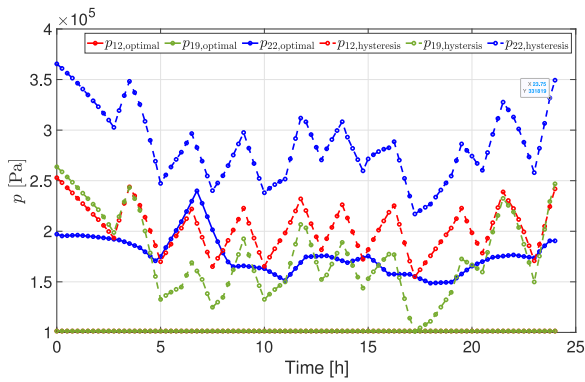


Fig. 9. Baseline and computed optimal profiles of pressure in WDS end-points.

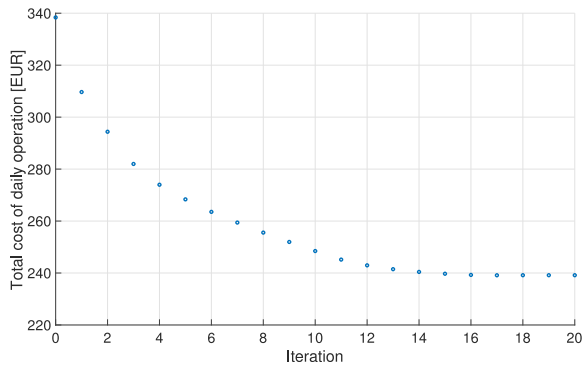


Fig. 10. Total cost of daily operation of the WDS through iterations of the optimization procedure.

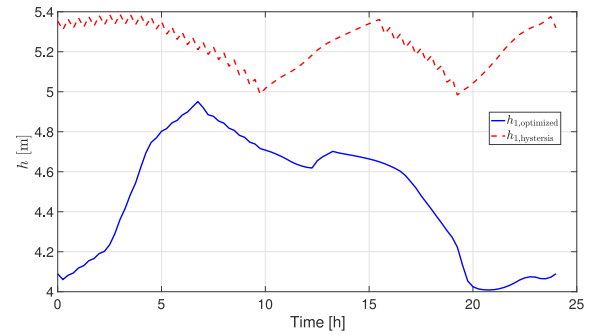


Fig. 11. Comparison of height profiles in the first tank obtained using SLP and baseline control.

where $\text{var}(d_b)$, is the variance of the diameters of all pipes that meet at node $n \in \mathcal{N}_{\text{loss}}$, and k_{loss} is the proportionality coefficient. The dimensions of all states, control inputs, and disturbances for the WDS segment of a city in Spain are presented in Table B.6, located in the Appendix B. All other parameters of the considered network from Table 1 are directly obtained from the EPANET file after transferring the data from GIS to the EPANET file. Again, hysteresis control was used as the baseline operation. In this scenario, seven flow-driven pumps operate in parallel, turning on and off based on the level in one of the tanks. The pumps are switched off when the water level exceeds 3.75 m and activated when it drops below 3.2 m. The remaining flow-driven pump is activated or deactivated based on the water levels in the six main adjacent tanks. That is, the pump is deactivated when the water level in any of the six tanks exceeds 5.8 m, and activated when the water level drops below 5 m. The pump activation and deactivation thresholds are selected to guarantee positive pressures throughout the network and to prevent pressures at end-points from dropping below the minimum overpressure threshold, i.e., 1 bar. In hysteresis control, the settings of the PBVs and the PDP are assumed to remain constant throughout the day. In this case study, the simulation was also repeated for several consecutive days, utilizing a repeating disturbance sequence until a steady-state diurnal harmonic behaviour was achieved. This was done to ensure a valid comparison with the SLP.

5.4. SLP operation on WDS segment of a city in Spain

As with the toy-example case study, the optimization procedure is started from the response of the system subject to baseline operation. The comparison of water levels in the first tank is shown in Fig. 11. Furthermore, comparison of the optimal input flow profiles and baseline control for an individual pump and for one of the seven pumps in parallel configuration are shown in Figs. 12 and 13, respectively. The optimal PBV pressure drop profile and baseline control profile for one of the PBVs are shown in Fig. 14. Comparison of the optimal pump difference pressure profile and baseline control profile for the PDP is shown in Fig. 15. Fig. 16 shows overpressure at one node where the constraint is defined that the overpressure must be greater than or equal to 1 bar. That node is located downstream of the PBV to provide additional validation of the valve's settings. Total cost of daily operation of the WDS through iterations of the optimization procedure is shown in Fig. 17. The cost value at iteration zero represents the cost associated with the baseline operation. Finally, comparison of costs due to water leakage and electricity consumption as well as comparison of the total daily operation costs of the city WDS segment considered is shown in Table 3.

The relative total cost savings using the SLP procedure compared to hysteresis control is 38.68%. The procedure was performed on the same computer platform as for the toy-example. The execution time for the whole optimization procedure including all the iterations shown as well as generating the model structure in MATLAB from the description file, is 1 h and 4 min.

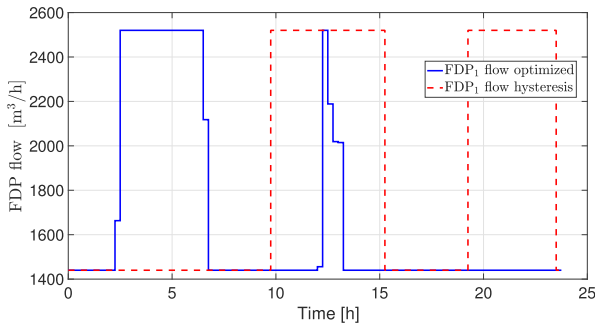


Fig. 12. Baseline and the optimal computed input flow for the individual FDP.

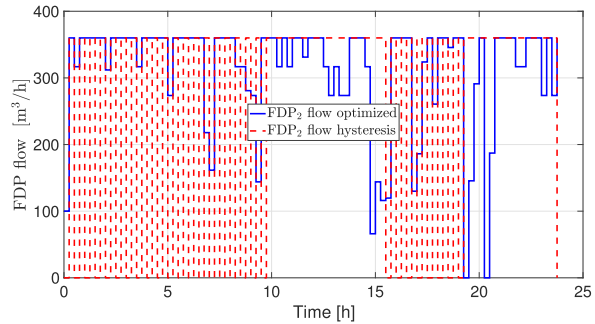


Fig. 13. Baseline and the optimal computed input flow for one of the FDPs located in parallel.

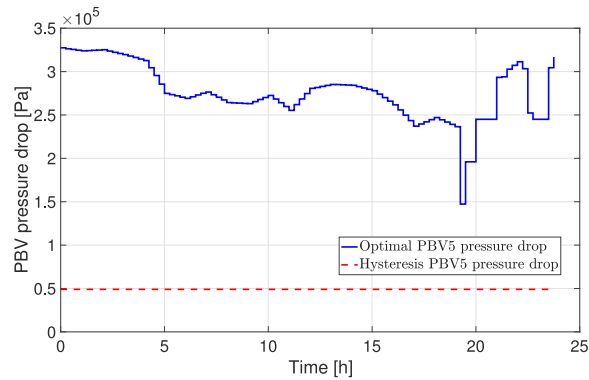


Fig. 14. Baseline and optimal PBV pressure drop profile for one of the PBVs.

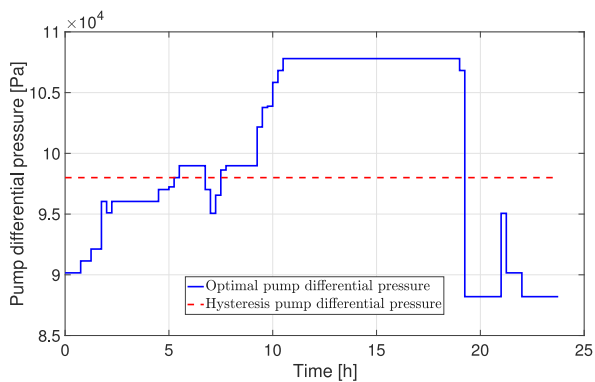


Fig. 15. Baseline and optimal pump pressure difference profiles.

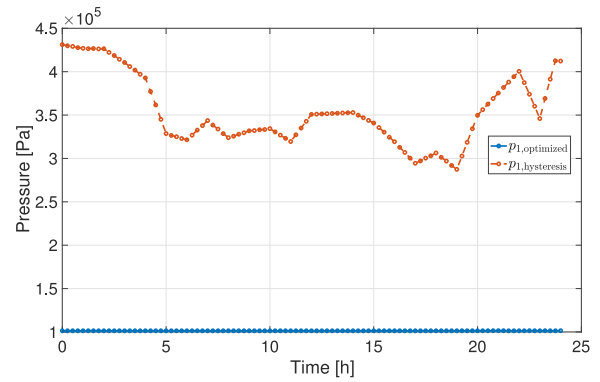


Fig. 16. The overpressure at a node after the PBV.

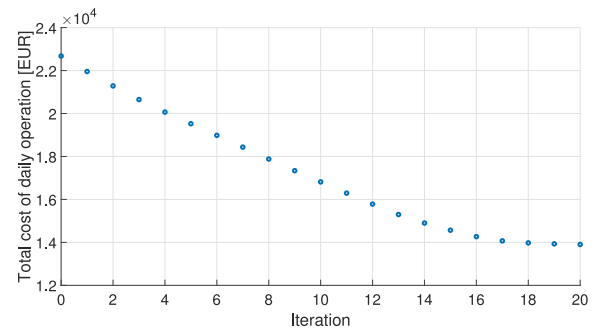


Fig. 17. Total cost of daily operation of the WDS through iterations of the optimization procedure.

Table 3

Daily cost comparison for a WDS segment within a city in Spain.

	Overall cost for lost water [EUR]	Overall cost for electricity [EUR]	Total cost [EUR]
Baseline	18 286	4390	22 676
SLP	10 584	3320	13 904

Table 4

Daily cost comparison for a WDS segment within a city in Spain.

	Overall cost for lost water [EUR]	Overall cost for electricity [EUR]	Total cost [EUR]
Advanced baseline	18 272	4027	22 299
SLP	10 225	3298	13 523

5.5. Comparison of advanced baseline and SLP operation on WDS segment of a city in Spain

In addition, as a baseline control, a scenario is created in which the hysteresis control takes into account the price of electricity as an additional condition. The scenario is designed so that the pumps are only turned off when the tanks are fully filled during periods of lower electricity prices. Also, in the period of lower electricity prices, the pumps are switched on at half of the minimum and maximum allowed water level in the tank. During periods of higher electricity prices, the pumps are activated only when the tank reaches the minimum allowable level and are turned off once the tank reaches halfway between the minimum and maximum allowable levels. For pumps located at the tank outlet, the logic for switching them on and off is reversed compared to the previously described logic for pumps positioned at the tank entrance. Comparison of costs due to water leakage and electricity consumption as well as comparison of total costs is shown in Table 4.

Using the described advanced baseline operation, total electricity costs are 363 EUR lower compared to the baseline operation described

in Section 5.3, confirming that some savings occurred. The optimization procedure is once again initiated using the system's response under the advanced baseline operation. The relative total cost savings using the SLP procedure compared to the described advanced baseline operation is 39.36%. The significant potential of the approach is demonstrated by this result, with even greater relative cost savings achieved in this case due to the convergence to a different local minimum.

6. Conclusion

Predictive control via sequential linear programming for a general water distribution system (WDS) is introduced. A general water distribution network setup is elaborated in the paper along with the mathematical model in the general form. The WDS linearization procedure for its general structure is explained in detail. The operating costs of the WDS are introduced, which are locally minimized while meeting all requirements. The procedure was validated on a toy-example and on a WDS segment of a city in Spain. The savings are substantial, both in terms of electricity costs and lost water costs, indicating significant economical potential for the implementation of the described procedure on larger water distribution systems.

CRedit authorship contribution statement

Blař Korotaj: Writing – original draft, Visualization, Validation, Software, Methodology, Investigation, Formal analysis, Data curation. **Mario Vařak:** Writing – review & editing, Validation, Supervision, Software, Project administration, Methodology, Funding acquisition, Conceptualization.

Declaration of competing interest

The authors declare that they have no known competing financial interests or personal relationships that could have appeared to influence the work reported in this paper.

Appendix A. Nodes and branches sets for WDS in Fig. 2

For the WDS in Fig. 2, the sets \mathcal{N} , $\mathcal{N}_{\text{storage}}$, \mathcal{N}_{HPD} , \mathcal{N}_{PDN} , $\mathcal{N}_{\text{pressure}}$ and $\mathcal{N}_{\text{loss}}$ are defined as the following sets of integers:

$$\mathcal{N} = \{1, 2, 3, 4, 5, 6, 7, 8, 9, 10, 11, 12, 13, 14, 15, 16, 17, 18, 19, 20, 21, 22, 23\}, \quad (\text{A.1})$$

$$\mathcal{N}_{\text{storage}} = \{4, 16\}, \quad (\text{A.2})$$

$$\mathcal{N}_{\text{HPD}} = \{12, 19, 23\}, \quad (\text{A.3})$$

$$\mathcal{N}_{\text{PDN}} = \{1\}, \quad (\text{A.4})$$

$$\mathcal{N}_{\text{pressure}} = \{11, 12, 19, 23\}, \quad (\text{A.5})$$

$$\mathcal{N}_{\text{loss}} = \{5, 9, 15\}. \quad (\text{A.6})$$

The sets of branches \mathcal{B} , \mathcal{B}_{FDP} , \mathcal{B}_{PBV} , \mathcal{B}_{PDP} , $\mathcal{B}_{\text{flow}}$, \mathcal{B}_{cf} and \mathcal{B}_{of} as the sets of ordered pairs of two neighbouring nodes are defined as:

$$\begin{aligned} \mathcal{B} = \{ & (1, 2), (2, 3), (3, 4), (4, 5), (5, 6), (6, 7), (7, 8), \\ & (8, 9), (9, 10), (10, 11), (11, 12), (9, 12), (5, 13), \\ & (13, 14), (14, 15), (15, 16), (15, 17), (17, 18), (18, 19), \\ & (15, 20), (20, 21), (21, 22), (22, 23)\}, \end{aligned} \quad (\text{A.7})$$

$$\mathcal{B}_{\text{FDP}} = \{(2, 3), (13, 14)\}, \quad (\text{A.8})$$

$$\mathcal{B}_{\text{PBV}} = \{(7, 8)\}, \quad (\text{A.9})$$

$$\mathcal{B}_{\text{PDP}} = \{(21, 22)\}, \quad (\text{A.10})$$

$$\mathcal{B}_{\text{flow}} = \{(10, 11)\}, \quad (\text{A.11})$$

$$\mathcal{B}_{\text{cf}} = \{(2, 3), (10, 11), (13, 14)\}, \quad (\text{A.12})$$

Table B.5

State-space model dimensions for the toy-example.

	Variable	Dimensions
States	$(h_n)_{n \in \mathcal{N}_{\text{storage}}}$	1
Inputs	$(q_{\text{FDP},b})_{b \in \mathcal{B}_{\text{FDP}}}$	2
	$(\Delta p_{\text{PBV},b})_{b \in \mathcal{B}_{\text{PBV}}}$	1
	$(\Delta p_{\text{PDP},b})_{b \in \mathcal{B}_{\text{PDP}}}$	1
Disturbances	$(D_{\text{dem},n})_{n \in \mathcal{N}_{\text{HPD}}}$	10
	$(p_n)_{n \in \mathcal{N}_{\text{PDN}}}$	1
Outputs	$(p_n)_{n \in \mathcal{N}_{\text{pressure}}}$	20
	$(q_b)_{b \in \mathcal{B}_{\text{flow}}}$	18
	$(q_{\text{loss},n})_{n \in \mathcal{N}_{\text{loss}}}$	5
	$(S_{\text{FDP},b})_{b \in \mathcal{B}_{\text{FDP}}}$	2
	$(S_{\text{PDP},b})_{b \in \mathcal{B}_{\text{PDP}}}$	1

Table B.6

State-space model dimensions for the WDS segment of a city in Spain.

	Variable	Dimensions
States	$(h_n)_{n \in \mathcal{N}_{\text{storage}}}$	10
Inputs	$(q_{\text{FDP},b})_{b \in \mathcal{B}_{\text{FDP}}}$	8
	$(\Delta p_{\text{PBV},b})_{b \in \mathcal{B}_{\text{PBV}}}$	8
	$(\Delta p_{\text{PDP},b})_{b \in \mathcal{B}_{\text{PDP}}}$	1
Disturbances	$(D_{\text{dem},n})_{n \in \mathcal{N}_{\text{HPD}}}$	631
	$(p_n)_{n \in \mathcal{N}_{\text{PDN}}}$	1
Outputs	$(p_n)_{n \in \mathcal{N}_{\text{pressure}}}$	6992
	$(q_b)_{b \in \mathcal{B}_{\text{flow}}}$	7380
	$(q_{\text{loss},n})_{n \in \mathcal{N}_{\text{loss}}}$	728
	$(S_{\text{FDP},b})_{b \in \mathcal{B}_{\text{FDP}}}$	8
	$(S_{\text{PDP},b})_{b \in \mathcal{B}_{\text{PDP}}}$	1

$$\begin{aligned} \mathcal{B}_{\text{of}} = \{ & (1, 2), (3, 4), (4, 5), (5, 6), (6, 7), (7, 8), \\ & (8, 9), (9, 10), (11, 12), (9, 12), (5, 13), \\ & (14, 15), (15, 16), (15, 17), (17, 18), (18, 19), \\ & (15, 20), (20, 21), (21, 22), (22, 23)\}. \end{aligned} \quad (\text{A.13})$$

Specific ordered pair from the set \mathcal{B} in (A.7) is also assigned with a unique integer to represent a branch with a single branch integer index, for easier notation.

Appendix B. State-space model dimensions for the case studies

The dimensions of the state-space model for the toy example are shown in Table B.5, while those for the WDS segment of a city in Spain are presented in Table B.6.

References

- Abdulrahman, A., & Nasher, N. (2010). Water supply network system control based on model predictive control. *Journal of King Saud University (Engineering Sciences)*, 22(2), 119–126.
- Archibald, T. W., & Marshall, S. E. (2018). Review of mathematical programming applications in water resource management under uncertainty. *Environmental Modeling & Assessment*, 23(6), 753–777.
- Baunsgaard, K. M. H., Ravn, O., Kalleřoe, C. S., & Poulsen, N. K. (2016). MPC control of water supply networks. In *Proc. of the 2016 European Control Conference* (pp. 1770–1775).
- Berkel, F., Caba, S., Bleich, J., & Liu, S. (2018). A modeling and distributed MPC approach for water distribution networks. *Control Engineering Practice*, 81, 199–206.
- Cembrano, G., Wells, G., Quevedo, J., P3rez, R., & Argelaguet, R. (2000). Optimal control of a water distribution network in a supervisory control system. *Control Engineering Practice*, 8, 1177–1188.
- Ciminski, A., & Duzinkiewicz, K. (2017). Direct algorithm for optimizing robust MPC of drinking water distribution systems hydraulics. In *Proc. of the 2017 22nd International Conference on Methods and Models in Automation and Robotics* (pp. 13–18).
- Engell, S. (2007). Feedback control for optimal process operation. *Journal of Process Control*, 17(3), 203–219.
- Fooladivanda, D., & Taylor, J. A. (2018). Energy optimal pump scheduling and water flow. *IEEE Transactions on Control of Network Systems*, 5(3), 1016–1026.

- Goryashko, A., & Nemirovski, A. (2014). Robust energy cost optimization of water distribution system with uncertain demand. *Automation and Remote Control*, 75, 1754–1769.
- Martinez, C. O., Puig, V., Cembrano, G., & Quevedo, J. (2013). Application of predictive control strategies to the management of complex networks in the urban water cycle. *IEEE Control Systems Magazine*, 33(1), 15–41.
- Menke, R., Abraham, E., Parpas, P., & Stoianov, I. (2016). Demonstrating demand response from water distribution system through pump scheduling. *Applied Energy*, 170, 377–387.
- Muranho, J., Ferreira, A., Sousa, J., Gomes, A., & Marques, A. (2020). Pressure-driven simulation of water distribution networks: Searching for numerical stability. In G. Corfu (Ed.), *Environmental Sciences Proceedings*, 48.
- Press, W. H., Teukolsky, S. A., Vetterling, W. T., & Flannery, B. P. (2007). *Numerical Recipes 3rd Edition: the Art of Scientific Computing*. USA: Cambridge University Press.
- Rawlings, J., Mayne, D. Q., & Diehl, M. (2017). *Model Predictive Control: Theory, Computation, and Design*. Santa Barbara, CA: Nob Hill Publishing.
- Rossman, L. A., Woo, H., Tryby, M., Shang, F., Janke, R., & Haxton, T. (2020). *EPANET 2.2 User Manual*. U.S. Environmental Protection Agency.
- Shao, Y., Zhou, X., Yu, T., Zhang, T., & Chul, S. (2024). Pump scheduling optimization in water distribution system based on mixed integer linear programming. *European Journal of Operational Research*, 313, 1140–1151.
- Shiu, C.-C., Chiang, T., & Chung, C.-C. (2022). A modified hydrologic model algorithm based on integrating graph theory and GIS database. *Water*, 14(19), 3000.
- Sun, C. C., Puig, V., & Cembrano, G. (2014). Combining CSP and MPC for the operational control of water networks: Application to the Richmond case study. *IFAC Proceedings Volumes*, 47(3), 6246–6251.
- Van Zyl, J. E., & Clayton, C. R. I. (2007). The effect of pressure on leakage in water distribution systems. *Proceedings of the Institution of Civil Engineers - Water Management*, 160(2), 109–114.
- Vašak, M., & Novak, H. (2019). Optimal control for daily operation planning of a water distribution system with pumped storage. In *Proc. of the 5th International Conference on Power Generation Systems and Renewable Energy Technologies* (pp. 1–6).

Vieira, B. S., Mayerle, S. F., Campos, L. M., & Coelho, L. C. (2020). Optimizing drinking water distribution system operations. *European Journal of Operational Research*, 280, 1035–1050.

Wang, Y., Ocampo-Martinez, C., & Puig, V. (2015). Robust model predictive control based on Gaussian processes: application to drinking water networks. In *Proc. of the 2015 European Control Conference* (pp. 3292–3297).



Blaž Korotaj received the M.Sc. degree from the University of Zagreb Faculty of Electrical Engineering and Computing (UNIZG-FER), Zagreb, Croatia, in 2020. Currently, he is Ph.D. student and a Researcher with the Department of Control and Computer Engineering and a member of the Laboratory for Renewable Energy Systems at UNIZG-FER. His current research interests focus on dynamic systems predictive control with applications to water distribution systems and drinking water treatment plants.



Mario Vašak received the Ph.D. degree from the University of Zagreb Faculty of Electrical Engineering and Computing (UNIZG-FER), Zagreb, Croatia, in 2007. He is currently a Full Professor Tenure with the Department of Control and Computer Engineering, UNIZG-FER, and the Head of the Laboratory for Renewable Energy Systems at UNIZG-FER. He has authored more than 30 articles in international scientific journals and overall more than 100 internationally reviewed articles. His current research interests are in the domain of dynamic systems predictive control with applications to green energy systems, buildings and critical infrastructure. He was the President of the Control Systems Chapter of the IEEE Croatia Section from 2014 to 2017.